Development of an optical measuring technique for the study of acoustical phenomena

J. M. Buick, J. A. Cosgrove, D. M. Campbell and C. A. Greated

Department of Physics and Astronomy, JCMB, The University of Edinburgh, Mayfield Road Edinburgh EH9 3JZ, UK

Abstract

We consider the application of optical methods to the measurement of acoustical phenomena. In particular we consider the suitability of applying measuring techniques that rely on the flow being seeded with small particles. This is a common practice when acoustic fields are not present, however, interactions between the seeding particles and the sound waves can change both the motion of the particles and any acoustically generated flow. The novel measuring technique of Fluorescent Dye Velocimetry is proposed which does not require the flow to be seeded. The accuracy and applicability of the new technique is then assessed using simulated images.

1 Introduction

Optical measuring techniques are now widely applied to flow measurement in a range of applications in fluid mechanics. One significant advantage that optical measuring techniques have compared to other methods is that they are considered to be non-intrusive; that is, there is no probe or measuring device inserted in the fluid and so the procedure of making a measurement does not alter the system in any way. However, many techniques, such as particle image velocimetry (PIV) and laser Doppler anemometry (LDA), rely on small seeding particles being present in the fluid. Provided these particles follow the flow in a reliable manner they are not considered to influence the fluid motion. This is generally true, however, when an acoustical field is present a number of problems can arise. Firstly, the action of the sound waves can move the particles at a different speed from the surrounding fluid and thus preventing an accurate velocity measurement from being taken.

Secondly, the particles can alter the acoustic field. This means that any flow that is derived from the acoustic field will be changed by the addition of the seeding particles. The first of these problems has already been addressed [1] by considering the radiation stress acting on the seeding particles. A suitable seeding particle is then selected so that its deviation from the fluid motion is negligible. This will be described briefly in section 2. In the remainder of the paper we propose and evaluate a new optical technique: Fluorescent Dye Velocimetry (FDV). This uses a fluorescent dye which diffuses at a molecular level and so there are no seeding particles to interact with the sound field.

2 Radiation Stress

Consider an acoustical wave propagating through a fluid which contains a number of suspended particles. If there is a mismatch between the acoustic impedance of the fluid and a suspended particle, then the wave will experience a strong reflection at the particle. This causes a large spatial change in the energy density and a large radiation pressure. The effect of this radiation force on a seeding particle has already been investigated [1]. If the density of the seeding particle, ρ_1, is similar to the density of the fluid, ρ_0, such that $\Lambda \to 1$, where $\Lambda = \rho_0 / \rho_1$ and $x_0 = kR \ll 1$, where R is the radius of the particle and k is the wavenumber of a plane progressive wave, then the radiation stress is given by [2,3]

$$F_{rs} = 2\pi\rho_0 |A|^2 x_0^6 \frac{\left[1 + 2(1-\Lambda)^2/9\right]}{(2+\Lambda)},$$

where A is given by

$$A = \sqrt{\frac{2I}{\rho_0 k \omega}},$$

ω is the angular frequency and I is the probe intensity. Now, the motion of a spherical seeding particle moving under the action of the radiation stress force F_{rs} and Stoke's drag force $-6\pi\mu R v$, where μ is the fluid viscosity and v is the velocity of the particle relative to the fluid, is described by

$$\frac{\mathrm{d}v}{\mathrm{d}t} = \frac{F_{rs}}{m} - \frac{6\pi\mu R v}{m},$$

where m is the particles mass. Following [1] the particle terminal velocity can be found by integrating and letting $t \to \infty$, which gives

$$v_\infty = \frac{F_{rs}}{6\pi\mu R}.$$

The magnitude of the terminal velocity depends on the radius of the particle as

$$v_\infty \propto R^5.$$

Thus the value of v_∞ is reduced rapidly with decreasing R and so the seeding particles will follow the flow provided R is small enough that v_∞ is negligible with respect to the fluid velocity.

3 Fluorescent Dye Velocimetry

In this section we consider a new optical technique FDV for velocity measurement in acoustic flows.

3.1 Motivation

If the seeding particles are selected according to the criteria outlined in section 2, it is clear that the particles will follow the flow to a desired degree of accuracy. The acoustic field, however, will still experience a small reflection at each particle; the cumulative effect of which could still be large. When measuring flows such as acoustic streaming which is produced solely by the attenuation of the acoustic field, any change in the acoustic field due to the seeding particles will inevitably change the fluid motion. It is therefore important to ensure that the measured (seeded) flow is not significantly different from the unseeded flow. Here we consider a new measuring technique in which a dye is added to the fluid rather than seeding particles. The dye diffuses on a molecular level and so will not alter the acoustic field.

3.2 Image Capture

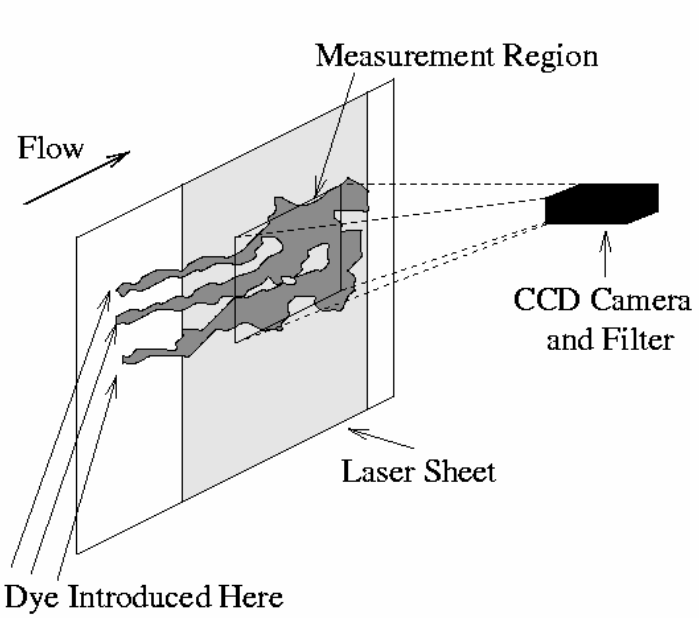

Figure 1: Experimental setup for obtaining FDV images

Figure 1 shows a typical experimental set up for obtaining FDV images. Fluorescent dye, for example Rhodamine B, is introduced into the flow upstream of the measurement region. This must be done in such a way what any velocity with which the dye is injected into the flow has dissipated by the time the dye reached the measurement region. It is also important that the dye has mixed sufficiently so that it occupies a significant fraction of the measurement region, but not to the extent that it is evenly mixed.
The measurement region is illuminated with a laser sheet at the frequency at which the dye

fluoresces. The fluorescence is then captured by a CCD camera through an optical filter which removes the laser light and transmits the fluorescent light. A pair of images taken at a short time separation are required for the analysis. Methods for inserting the dye, producing the light sheet and obtaining the images will vary depending on the application. Illumination and image capture techniques widely applied in PIV [4,5] can also be applied to FDV.

3.3 Simulated Images

To test the effectiveness of the new technique a number of simulated images were created. To do this a pair of images must be generated in which the dye configuration in the second image has been shifted slightly with respect to its position in the first; corresponding to two images of a real dye system taken with a short time separation. This was done using a random walk routine on a 6400 by 6400 grid. Starting at the centre of the grid a series of 5000 points were generated using a random walk with a Gaussian distribution with mean 0.0 and standard deviation of 128 points. If the random point lies outside the grid, the sequence is continued and future points which lie on the grid are considered. The sequence of points was then jointed by a series of straight lines. Two sets
of random walks are shown in figure 2. An intensity level, L, at each point on the grid was then calculated by fitting a Gaussian about each line according to the formula

$$L = 3.0\exp(-d^2/30^2),$$

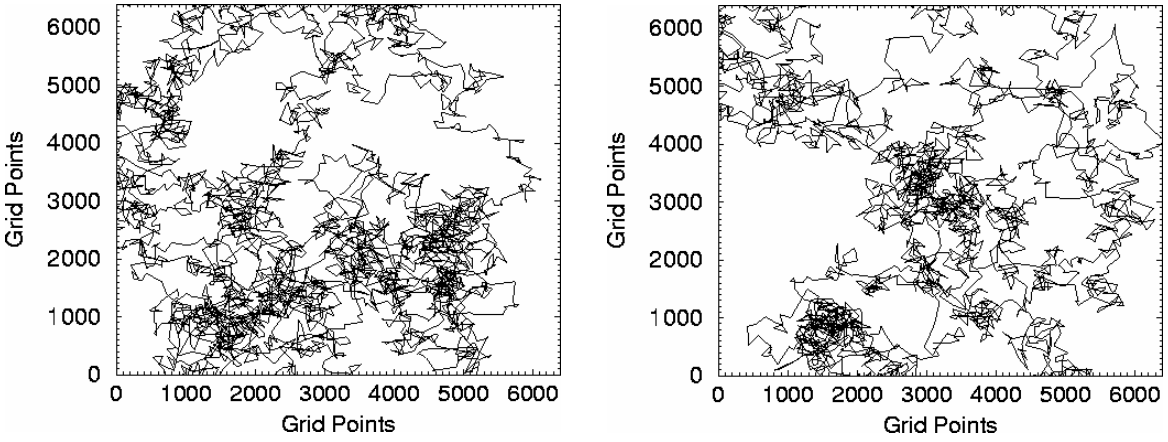

Figure 2: Random walks.

where d is the shortest distance between the grid point and the lines. The final intensity for each grid point was the sum of the contributions to L from each of the random walk lines. The grid was then divided into a 640 by 640 array of pixels, each pixel containing 10 by 10 grid points. The pixel intensity was found by summing the intensity level of each of the grid points making up the pixel and taking the integer part. This takes account of the averaging effect of the CCD camera. If the pixel intensity is greater than 255 it is set to a threshold value of 255 as would happen to an image taken by a CCD camera with 256 grey levels. The simulated FDV image produced for two of the random walks are shown in figures 3a and 3b. Using this system it is possible to impose any desired shift on the original grid to a resolution of 1 grid point, corresponding to 0.1 pixel. If the shift

corresponds to an integral number of pixels, then the pixel intensities will be the same in the two images, the only difference will be in the position. If, however, a non-integral pixel shift is applied, then the two images will be different due to the averaging procedure.

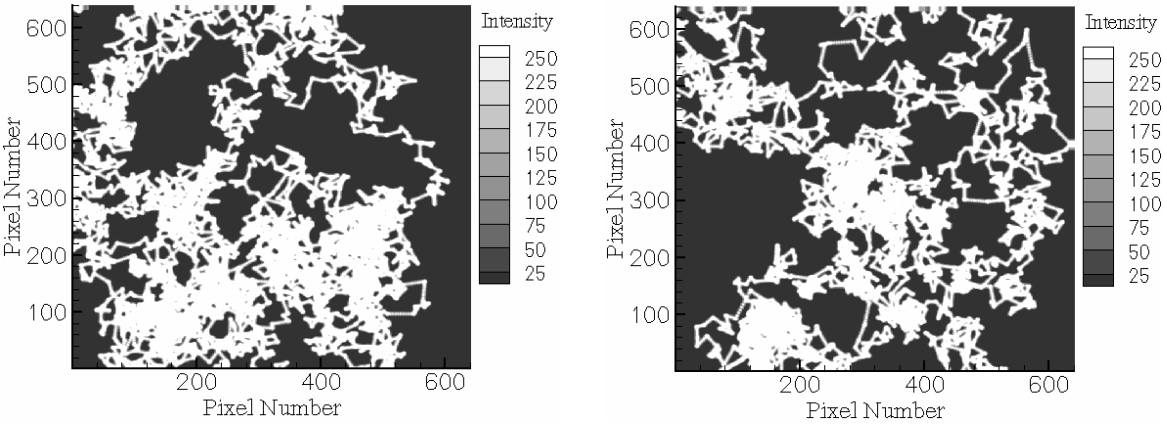

(a) Random seed 1 (b) Random seed 2

Figure 3: Simulated FDV images for two of the random seeds considered

3.4 Analysis of Images

The next stage of the process is to obtain velocity information from the FDV images. Each velocity vector was found by considering an interrogation region consisting of a 64 by 64 pixel area of the simulated image. A cross-correlation routine was applied to the original and shifted image and the peak value in the correlation plane determined. As with all digital correlations this introduces a bias error due to the windowing method. This bias [5,6] is in the form of the correlation of two square window functions and can be divided out of the computed correlation to give the correct correlation values from which a peak can be identified. This peak gives the displacement between the two simulated images to integer accuracy. As in PIV, the position of the peak in the correlation plane was determined to sub-pixel accuracy using a three-point estimator [6]. Different estimators can be applied depending on the shape of the peak, in the results presented here a Gaussian fit was applied and was found be satisfactory.

We note that, as the shift imposed on the second image is increased, the area of overlap between the two images is reduced. To overcome this a second phase of the analysis can be performed. The original interrogation region of the first image is correlated with an interrogation region from the second image which is displaced by an amount $(-m,-n)$ from its position in the initial analysis, where m and n are the closest integers to the two-component displacement obtained from the first phase of the analysis. If the second phase gives a real displacement (using the Gaussian fit estimator) which is (x',y'), then the final displacement is given as $(x,y) = (m,n)+(x',y')$. This second phase of analysis is known

as reinterrogation.

Since we are dealing here with simulated images we are content to consider the measured displacement and compare it to the known shift, thus enabling us to consider the accuracy of the technique. When real images are analysed the velocity is obtained by dividing the displacement by the time separation of the images.

3.5 Results

In this section we present results obtained using the simulated images and consider aspects of the analysis. A total of five random seeds were used to produce 5 pairs of FDV images, each 640 by 640 pixels. Interrogation regions were selected every 32 pixels (note that there is an overlap between adjacent regions) giving 19 x 19 interrogation regions per image pair. The maximum number of data points obtained for each shift is therefore 5 x 19 x 19 = 1,805. In practice the number of data points obtained was slightly smaller since, for example, it is not always possible to find a suitable region for reinterrogation if the original is at the edge of the image.

3.5.1 Reinterrogation

Figure 4 shows the percentage of displacements which were calculated correctly within a tolerance of 0.5 pixels, with and without reinterrogation, for shifts of 0.0, 1.0, 3.0, 6.0, 9.0 and 12.0 pixels along the *x*-axis. In each case there was no shift along the *y*-axis. For both techniques the number of correct measurements is approximately 100 % for a shift of 0.0 pixels, that is when the two images are identical. For larger shifts the reinterrogation method shows a significant improvement giving an accuracy of over 85 % compared to an accuracy of about 20 % when there is no reinterrogation. The reason for this can be seen by comparing figures 5a and 5b which show the spread of measured displacements when the second image is shifted by 3.0 pixels. The results are plotted in the form of a histogram with box widths of 0.1 pixels. Figures 5a shows the results when reinterrogation is not applied. The distribution is approximately Gaussian in shape with the maximum occurring between 2.95 and 3.05 pixels, however, there is a slight bias towards lower values. In particular, there are a few measured values less than 2.5 but none greater than 3.5. The results in figure 5b are for reinterrogation. All interrogation regions which gave an initial measurement between 2.5 and 3.5 (figure 5a shows that this is a significant percentage of all the results) are reinterrogated by moving the second image by -3 pixels so that it coincides with the first image. From figure 4 we can see that approximately 100 % of the interrogation regions give the correct displacement (to within ± 0.05 pixels) when the two images coincide. Thus virtually all the results which originally lie between 2.5 and 3.5 are seen to give the correct answer (to within ± 0.05 pixels) after reinterrogation. In figure 5a we also see a few results which predict a displacement of slightly less then 2.5 pixels. There are a similar number of results in figure 5b with a displacement slightly less than 2.5; although the reinterrogated process will change the measured displacement it does not appear to significantly improve it in this region. The peak at a displacement of 3.0 pixels in figure 5b is about 85 %. The other 15 % of results include those below 2.5 pixels which are shown in the histogram and also about 10 % of the results predict a displacement close to 0.

These are not shown in the histogram and are mainly due to regions where the mean intensity is low. This will be discussed in the next section.

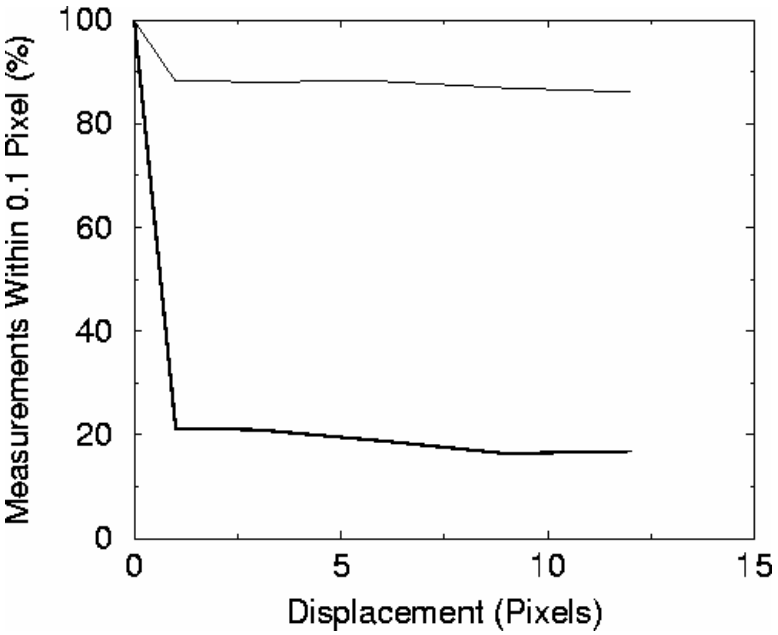

Figure 4: Percentage of displacements which were calculated correctly to within a tolerance of 0.05 pixels The thin and thick lines were obtained with and without reinterrogation respectively.

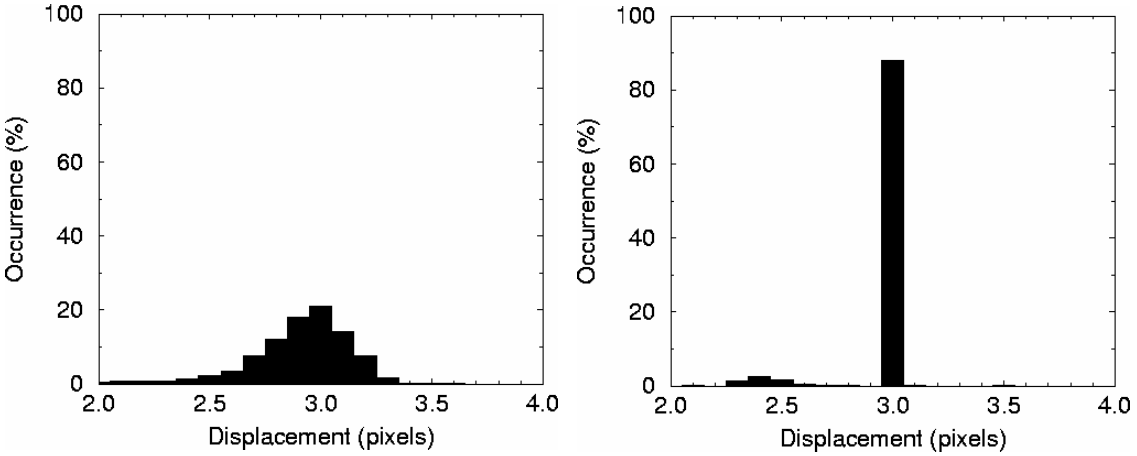

(a) No reinterrogation (b) Reinterrogation

Figure 5: Histograms showing the spread of measured displacement for a shift of 3.0 pixels, without (a) and with (b) reinterrogation.

3.5.2 Intensity Levels

The results presented above have shown that it is possible to use FDV to obtain a reasonable measurement of the displacement between images. We have seen that with reinterrogation we can obtain an answer correct to ± 0.05 pixels from about 85 % of interrogation regions. It is important to have a method for identifying regions which are likely to give a good or a poor measurement. One factor which is likely to be important here is the average intensity of the interrogation region. Some of the interrogation regions will contain no dye, in which case it will not be possible to obtain any velocity information for that portion of the image. However, even regions with only a small amount of dye, see for example figure 6a, can provide velocity information. Similarly, it is possible that there will be interrogation regions where all the pixel values will be 255 and again it will not be possible to obtain any information. In fact, such a region was not found for any of the random seeds used. Even in regions with a high mean density there were small regions with lower intensities, see figure 6b.

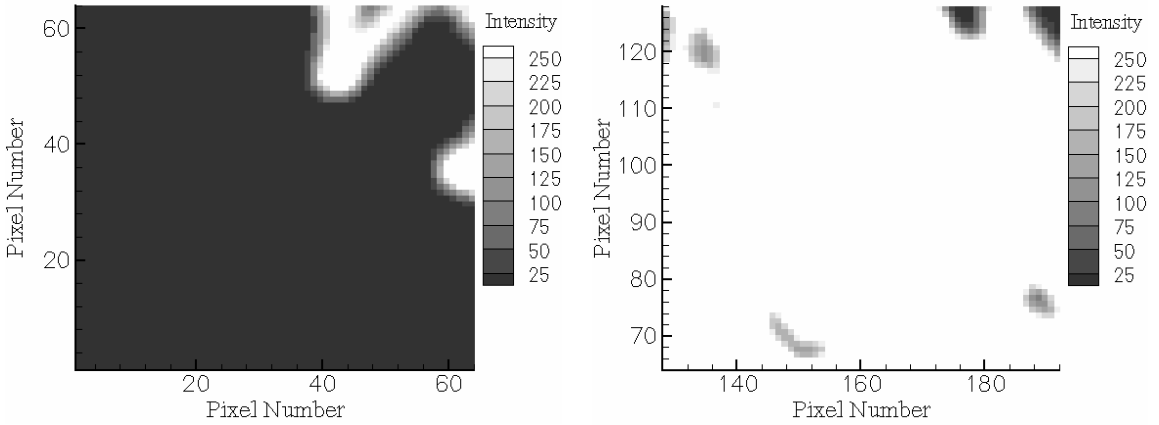

(a) Region with a low mean intensity (b) Region with a high mean intensity

Figure 6: Two interrogation regions taken from figure 3b.

To investigate this the measured displacement is plotted in figure 7 as a function of the mean intensity level in the interrogation region of the first image. The results are represented by dots, since the majority of them lie close to a displacement of 3.0 pixels they form an almost continuous line at this value. Also shown in the figure are the running mean calculated over twenty points and the corresponding running standard deviation. As the average intensity decreases from about 50 to zero bits per pixel, the deviation between the running mean and the shift value of 3.0 is seen to increase with many of the measured values significantly different from the shift value. It in noted that, in this region, the analysis tends to pick displacements which are smaller in magnitude than the known shift. In this region there is also a significant increase in the running standard deviation as the mean intensity approaches zero. A similar but much less significant effect is also noticed at high intensities as the mean intensity approached 255 bits per pixel. For the remaining intensities the running mean is close to the shift value and the corresponding standard deviation is small.

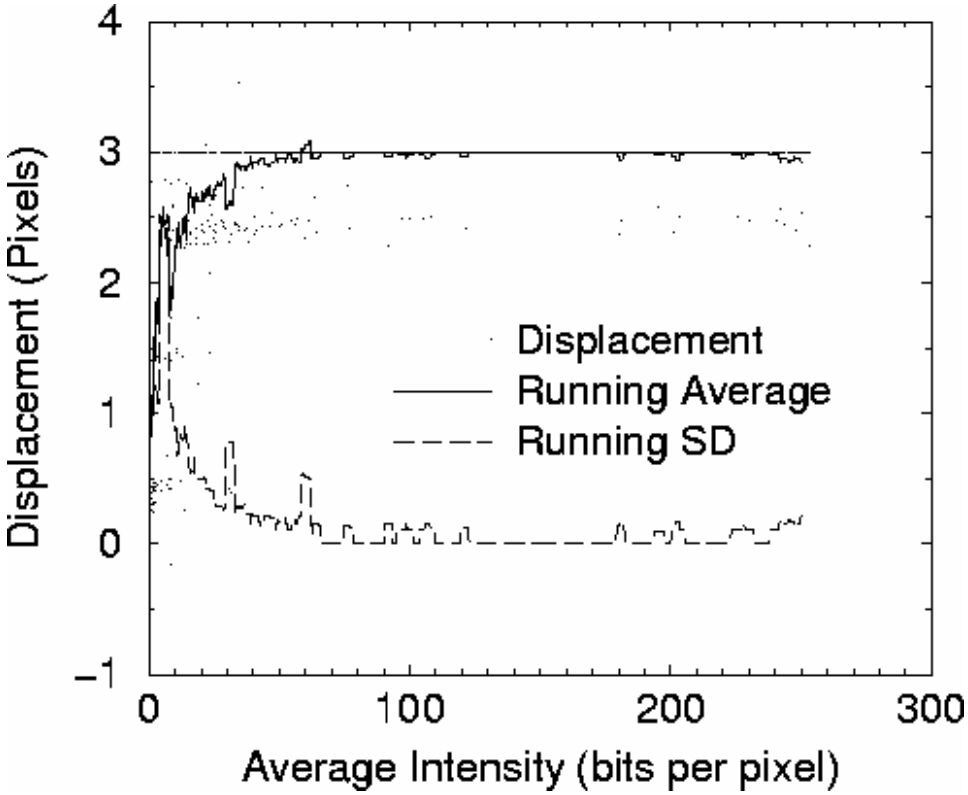

Figure 7: The measured displacement plotted as a function of the mean intensity of interrogation region. Also shown are running averages and running standard deviation calculated using 20 sequential points.

Figure 8 shows ΔM, the difference between the mean and the shift value, and σ, the standard deviation, found from all the results that have a mean density greater than 50 bits per pixel. The results are shown for shifts of 1.0, 3.0, 6.0, 9.0 and 12.0 pixels, with and without reinterrogation. The results suggest that provided the mean intensity is greater than 50 bits per pixel and we apply the reinterrogation algorithm we can obtain reliable displacement (and hence velocity) measurements for the integer shifts considered here. For each shift the mean measured displacement differs from the known shift by less then 0.1 pixels and the standard deviation is less then 0.02 pixels.

4 Conclusion

The application of optical measuring techniques to fluid flows associated with acoustical phenomena has been considered. In particular, consequences of introducing seeding particles into the flow are identified. The novel measuring technique Fluorescent Dye Velocimetry has been proposed. This involves introducing a fluorescent dye into the fluid. This dye diffuses at a molecular level and does not have the draw backs associated with traditional seeding particles. The new technique is then assessed using simulated images and it is seen that under certain circumstances FDV is capable of producing satisfactory results.

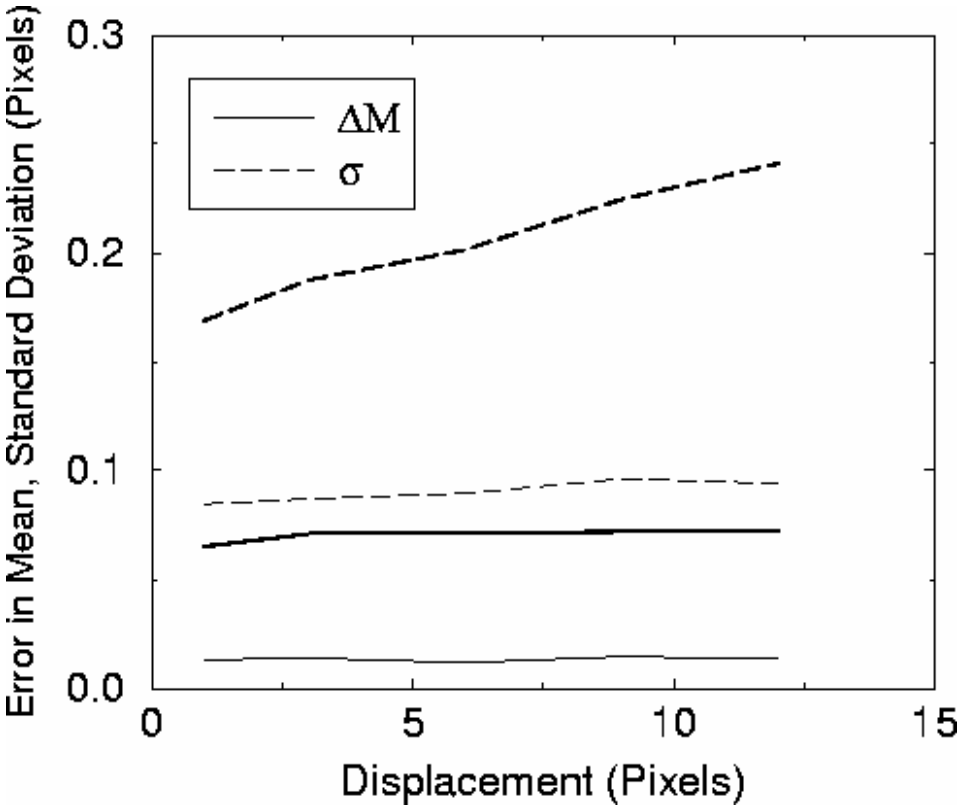

Figure 8: The mean and standard deviation for different image shifts with (thin) and without (thick) reinterrogation

References

[1] J. A. Cosgrove, J. M. Buick, D. M. Campbell, and C. A. Greated. PIV applied to acoustical phenomena. In *Proceedings of the 8th International Conference on Sound and Vibration*, pages 479 - 486, Hong Kong, China, 2001.

[2] L. V. King. On the acoustic radiation pressure on spheres. *Proceedings of the Royal Society of London A*, 147:212-240, 1934.

[3] A. A. Doinikov. Acoustic radiation pressure on a rigid sphere in a viscous fluid. *Proceedings of the Royal Society of London A,* 447:447-466, 1994.

[4] R. J. Adrian. Particle-imaging techniques for experimental fluid mechanics. *Annual Review of Fluid Mechanics*, 23:261-304, 1991.

[5] M. Raffel, C. Wilert and J. Kompenhans. *Particle Image Velocimetry - A Practical Guide*. Springer, 1998.

[6] J. Westerweel. *Digital Particle Image Velocimetry - Theory and Applications.* PhD thesis, Delft University, 1993.